Advances in Astronomy and Space Physics, **3**, 32-37 (2013)

Nonthermal emission model of isolated X-ray pulsar RX J0420.0-5022

N. Chkheidze[1]*, *Iu. Babyk*[2,3,4]†

[1]Center for Theoretical Astrophysics, ITP, Ilia State University, 0162, Tbilisi, Georgia
[2]Main Astronomical Observatory of NAS of Ukraine, 27 Akademika Zabolotnoho St., 03680 Kyiv, Ukraine
[3]Dublin Institute for Advanced Studies, Fitzwilliam Place, 31, Dublin 2, Ireland
[4]Dublin City University, Dublin 9, Ireland

In this paper, an alternative theoretical interpretation to the generally assumed thermal emission models of the observed X-ray spectrum of isolated pulsar RX J0420.0-5022 is presented. It is well-known that at a pulsar surface, the distribution function of relativistic particles is one-dimensional. However, cyclotron instability causes an appearance of transverse momenta of relativistic electrons, which as a result start to radiate in the synchrotron regime. On the basis of the Vlasov kinetic equation we study the process of quasi-linear diffusion (QLD) developed by means of the cyclotron instability. This mechanism enables the generation optical and X-ray emissions on the light cylinder lengthscales. An analysis of the three archival XMM-Newton observations of RX J0420.0-5022, is performed. Considering a different approach to synchrotron emission theory, a spectral energy distribution was obtained, which was in a good agreement with the observational data. A fit to the X-ray spectrum was conducted using both the present synchrotron emission model spectrum absorbed by cold interstellar matter, as well as the generally assumed black-body absorption model.

Key words: pulsars: individual RX J0420.0-5022, stars: magnetic fields, radiation mechanisms: non-thermal

INTRODUCTION

The soft X-ray source RX J0420.0-5022 (hereafter RX J0420) belongs to the group of seven radio-quiet, isolated neutron stars discovered in the ROSAT all-sky survey data, often referred to as the X-ray Dim Isolated Neutron Stars (XDINSs, see [10] for review). In the optical domain, only a few XDINSs have counterparts certified by their proper motion measurements. However several additional likely candidates remain, based on their coincidence with the X-ray positions [17]. The X-ray spectra of XDINSs are well-represented by an absorbed black-body model ($kT \approx 45 - 100\,\mathrm{eV}$), emission which originates in the hotter parts of the neutron star surface [10]. Whereas the cooler part of the XDINSs surface is assumed to be emitting in the optical domain [20]. The formation of a non-uniform surface temperature distribution is still under debate; it is most likely artificial and therefore needs to be examined through convincing theory. The optical emission is also explained in terms of hydrogen layers of finely-tuned thickness superposed on a condensed matter surface, reprocessing surface radiation [11], or in terms of non-thermal emission from particles in the star magnetosphere [18].

In contrast to somewhat contrived thermal emission models, the observed properties of the faintest object in X-rays among the XDINSs RX J0420 can be explained in the framework of the plasma emission model. This model has already been applied to explain the observed spectra of two other XDINSs (RX J1856.5-3754 and RBS1774, see [4, 5] for more details). The plasma emission model is based on the well-developed theory of pulsars [14, 15] and suggests successful interpretation of the observational data. According to these works, in the electron-positron plasma of a pulsar magnetosphere, the low frequency cyclotron modes, during the quasi-linear evolution stage, create conditions for generation of high energy synchrotron emission. Generally speaking, at the pulsar surface, relativistic particles efficiently lose their perpendicular momenta via synchrotron emission in very strong magnetic fields, therefore they transit to their ground Landau state very rapidly (pitch angles are vanishing). However, cyclotron instability causes the appearance of transverse momenta of relativistic particles in the outer parts of the pulsar magnetosphere. Therefore, the resonant electrons start to radiate in the synchrotron regime.

We suppose that the observed X-ray emission of RX J 0420 is generated by the synchrotron mechanism at the light cylinder length-scales. In general

*nino.chkheidze@iliauni.edu.ge
†babikyura@gmail.com

the synchrotron radiation spectrum is considered to be a power-law, which is not consistent with the observational data from RX J0420. The standard theory of the synchrotron radiation [2, 7] typically provides the power-law spectral energy distribution. Contrary to the standard scenario, by taking into account the specifications produced due to the present emission model we obtain different spectral distribution, which can be successfully fitted with the measured X-ray spectrum of RX J0420.

In this paper, we describe the plasma emission model and derive the synchrotron radiation spectrum based on our scenario, present the results of spectral analysis of re-processed XMM-Newton archival data from RX J0420, and present our conclusions.

EMISSION MODEL

Any well-known theory of pulsar emission suggests that the observed radiation is generated due to processes taking place in an electron-positron plasma. It is generally assumed that the pulsar magnetosphere consists of dense relativistic electron-positron plasma with an anisotropic one-dimensional distribution function (see Fig. 1 from [1]) and is comprised of the following components: a plasma bulk with an average Lorentz-factor of $\gamma_p \simeq 10^2$, a tail on the distribution function with $\gamma_t \simeq 10^5$, and the primary beam with $\gamma_b \simeq 10^7$. The distribution function is one-dimensional and anisotropic, hence the plasma becomes unstable, which may cause excitation of the plasma eigen-modes. Assuming the eigen-modes of the electron-positron plasma to have small inclination angles with respect to the magnetic field, one is left with three branches, two of which are mixed longitudinal-transversal waves ($lt_{1,2}$). The high frequency branch on the diagram $\omega(k_\parallel)$ begins with the Langmuir frequency and for longitudinal waves ($k_\perp = 0$), lt_1 reduces to the pure longitudinal Langmuir mode. The low frequency branch, lt_2, is similar to the Alfvén wave. The third t mode is the pure transversal wave, the electric component of which $\mathbf{E}^t$ is perpendicular to the plane of the wave vector and the magnetic field, $(\mathbf{k}, \mathbf{B}_0)$. The vector of the electric field $\mathbf{E}^{lt_1, lt_2}$ is located in the plane $(\mathbf{k}, \mathbf{B}_0)$. When $k_\perp = 0$, the t-mode merges with the lt waves and the corresponding spectra are given by [12]:

$$\omega_t \approx kc\,(1-\delta)\,, \qquad \delta = \frac{\omega_p^2}{4\omega_B^2\gamma_p^3}, \tag{1}$$

where k is the modulus of the wave vector, c is the speed of light, $\omega_p \equiv \sqrt{4\pi n_p e^2/m}$ is the plasma frequency, e and m are the electron's charge and rest mass, respectively, n_p is the plasma density, $\omega_B \equiv eB/mc$ is the cyclotron frequency, and B is the magnetic field induction.

The main mechanism of wave generation in plasmas of the pulsar magnetosphere is cyclotron instability. The cyclotron resonance condition can be written as [12]:

$$\omega - k_\parallel V_\parallel - k_x u_x + \frac{\omega_B}{\gamma_r} = 0, \tag{2}$$

where $u_x = cV_\varphi\gamma_r/\rho\omega_B$ is the drift velocity of the particles due to curvature of the field lines with a curvature radius ρ. During the wave generation process, one also has a simultaneous feedback of these waves on the resonant electrons [24]. This mechanism is described by the QLD, leading to a diffusion of particles along as well as across the magnetic field lines. Therefore, resonant particles acquire transverse momenta (pitch angles) and, as a result, start to radiate through the synchrotron mechanism.

The wave excitation leads to redistribution process of the resonant particles via the QLD. The kinetic equation for the distribution function of the resonant electrons can be written as [4]:

$$\frac{\partial f^0}{\partial t} + \frac{\partial}{\partial p_\parallel}\left\{F_\parallel f^0\right\} + \frac{1}{p_\perp}\frac{\partial}{\partial p_\perp}\left\{p_\perp F_\perp f^0\right\} = \\ = \frac{1}{p_\perp}\frac{\partial}{\partial p_\perp}\left\{p_\perp D_{\perp,\perp}\frac{\partial}{\partial p_\perp} f^0\,(\mathbf{p})\right\}, \tag{3}$$

where

$$F_\perp = -\alpha_s\frac{p_\perp}{p_\parallel}\left(1 + \frac{p_\perp^2}{m^2c^2}\right), \; F_\parallel = -\frac{\alpha_s}{m^2c^2}p_\perp^2 \tag{4}$$

are the transverse and longitudinal components of the synchrotron radiation reaction force and $\alpha_s = 2e^2\omega_B^2/3c^2$.

Here $D_{\perp,\perp}$ is the perpendicular diffusion coefficient, which can be defined as follows [4]:

$$D_{\perp,\perp} = \frac{e^2}{8c}\delta\,|E_k|^2\,, \tag{5}$$

where $|E_k|^2$ is the density of electric energy in the waves. Its value can be estimated from the expression $|E_k|^2 \approx mc^2 n_b\gamma_b c/2\omega$, where ω is the frequency of the cyclotron waves.

The transversal QLD increases the pitch-angle, whereas force $F_\perp$ resists this process, leading to a stationary state ($\partial f/\partial t = 0$). The pitch-angles acquired by resonant electrons during the process of the QLD satisfies $\psi = p_\perp/p_\parallel \ll 1$. Thus, one can assume that $\partial/\partial p_\perp >> \partial/\partial p_\parallel$. In this case the solution of Eq. (3) gives the distribution function of the resonant particles by their perpendicular momenta [4]:

$$f(p_\perp) = C\exp\left(\int\frac{F_\perp}{D_{\perp,\perp}}\mathrm{d}p_\perp\right) = Ce^{-\left(\frac{p_\perp}{p_{\perp 0}}\right)^4}, \tag{6}$$

where

$$p_{\perp_0} \approx \frac{\pi^{1/2}}{B\gamma_p^2}\left(\frac{3m^9c^{11}\gamma_b^5}{32e^6P^3}\right)^{1/4}. \quad (7)$$

And for the mean value of the pitch angle we find $\psi_0 \approx p_{\perp_0}/p_\parallel \simeq 10^{-3}$. Synchrotron emission is generated as the result of the presence of pitch angles.

SYNCHROTRON RADIATION SPECTRUM

To explain the observed X-ray emission of RXJ0420, let us assume that the resonant particles are the primary beam electrons with $\gamma_b \sim 10^7$, placing the synchrotron radiation in the soft X-ray spectrum. According to our emission scenario, the synchrotron radiation is generated as the result of acquirement of pitch angles by resonant particles, during the QLD stage of cyclotron instability. As was shown in [16], the cyclotron resonance condition (see Eq. (2)) is fulfilled at light cylinder lengthscales. Consequently, the observed X-ray emission comes from the region near the light cylinder, where the geometry of the field lines is determined by the curvature drift instability excited at the same lengthscales [19]. The curvature drift instability effectively rectifies the magnetic field lines (the curvature radius tends to infinity). Therefore, in the synchrotron emission generation region the field lines are practically straight and parallel to each other, and one can assume that electrons with $\psi \approx \psi_0$ efficiently emit in the observer's direction.

The synchrotron emission flux of the set of electrons in this case is given by (see [4]):

$$F_\epsilon \propto \int f_\parallel(p_\parallel) B\psi_0 \frac{\epsilon}{\epsilon_m}\left[\int_{\epsilon/\epsilon_m}^{\infty} K_{5/3}(z)\mathrm{d}z\right]\mathrm{d}p_\parallel. \quad (8)$$

Here $f_\parallel(p_\parallel)$ is the distribution function of the resonant electrons by their parallel momenta, $\epsilon_m \approx 5\cdot 10^{-12} B\psi\gamma^2\,\mathrm{keV}$ is a photon energy of maximum of the synchrotron spectrum of a single electron and $K_{5/3}(z)$ is the Macdonald function.

In order to find the synchrotron emission spectrum, one needs to know the behaviour of the distribution function, $f_\parallel(p_\parallel)$. For solving this problem, we consider the equation governing the evolution of $f_\parallel(p_\parallel)$ [4]:

$$\frac{\partial f_\parallel}{\partial t} = \frac{\partial}{\partial p_\parallel}\left(\frac{\alpha_s}{m^2c^2\pi^{1/2}} p_{\perp_0}^2 f_\parallel\right). \quad (9)$$

Considering the quasi-stationary case from Eq. (9), we can find the redistributed distribution function of the resonant particles by their parallel momenta:

$$f_\parallel \propto \frac{1}{p_\parallel^{1/2}\,|E_k|}. \quad (10)$$

On the other hand, the cyclotron noise is described by the equation

$$\frac{\partial |E_k|^2}{\partial t} = 2\Gamma_c |E_k|^2, \quad (11)$$

where

$$\Gamma_c = \frac{\pi^2 e^2}{k_\parallel} f_\parallel(p_r) \quad (12)$$

is the growth rate of the instability, and from the resonance condition (2) it follows that $k_\parallel \approx \omega_B/c\delta\gamma_r$. Combining Eqs. (9) and (11) it is easy to find that [4]:

$$|E_k|^2 \propto p_\parallel^{3-2n}, \quad (13)$$

here n denotes the index of the initial distribution function of the resonant electrons ($f_{\parallel_0} \propto p_\parallel^{-n}$). From Eqs. (10) and (13) it follows that $f_\parallel(p_\parallel) \propto p_\parallel^{n-2}$. As the emitting particles in our case are the primary beam electrons, nothing can be told about their initial distribution. We only know the scenario of creation of the primary beam electrons [8, 3] which are extracted from the pulsar's surface via the electric field induced by the star's rotation. To our knowledge there is no convincing theory that would predict the initial form of the distribution function of the beam electrons, which must be drastically dependent on the neutron star's surface properties and temperature.

The frequency of the original waves, excited during the cyclotron resonance can be estimated from Eq. (2) as follows

$$\nu \approx 2\pi\frac{\omega_B}{\delta\gamma_b} \sim 10^{14}\,\mathrm{Hz}. \quad (14)$$

As we can see, the frequency of the cyclotron modes comes in the same domain as the measured optical emission of XDINSs with the certified optical counterparts. Their spectra mostly follow the Rayleigh-Jeans tail $F_\nu \propto \nu^2$. On the other hand, the spectral distribution of the cyclotron modes is given by expression (13) and combining this equation with Eq. (14) we find

$$F_\nu \propto |E_k|^2 \propto \nu^{2n-3}. \quad (15)$$

From Eq. (15) it follows that when $n = 5/2$ the spectral distribution of the cyclotron modes is coincident with the Rayleigh-Jeans function. And for the initial distribution of the beam electrons, as well as for their final distribution, we find $f_{\parallel_0} \propto p_\parallel^{-5/2}$ and

$f_\parallel \propto p_\parallel^{1/2}$. We have used this distribution for the beam electrons to define the theoretical X-ray spectrum of RX J1856.5-3754, which fitted the measured one well [5]. Although for RX J0420 the detection of the optical counterpart has not yet been confirmed, based on similarities between XDINSs, we assume that the initial distribution function of the beam electrons must be the same for all XDINSs. Thus, in place of integral (8) as for two other XDINSs investigated in previous works [4, 5], we get:

$$F_\epsilon \propto \epsilon^{0.3} \exp\left[-(\epsilon/\epsilon_m)^b\right]. \qquad (16)$$

To find the values of the parameters b and ϵ_m, one should perform a spectral analysis by fitting the model spectrum absorbed by cold interstellar matter with the observed X-ray spectrum of RX J0420.

SPECTRAL ANALYSIS

To obtain the X-ray spectra of RX J0420 with the highest statistical quality, we used the EPIC-pn data collected from three XMM-Newton observations between December 2002 and January 2003. The archival XMM-Newton data were processed with the `Science Analysis Software (SAS)` version `11.0`. The X-ray spectra were grouped in spectral bins containing at least 30 photons. Subsequent spectral analysis was performed with `XSPEC V12.7.0`. The three EPIC-pn spectra fits of RX J0420 were performed simultaneously, and spectral analysis was limited to energies between 0.15 and 1.0 keV. Along with the plasma emission model proposed in the present work, we also examined the black-body model to compare the fit results.

THE BLACK-BODY MODEL

For the spectral analysis of EPIC-pn data for RX J0420 first we used an absorbed black-body model. We allowed only the black-body normalization to vary between the spectra of the individual observations, and fitted the temperature and amount of interstellar matter as common parameters. We found that the black-body model provided a reasonable fit, but with $N_H \sim 10^{18}\,\mathrm{cm}^{-2}$, which is not perfect. Thus, we set a lower limit for this parameter, which did not alter the fit quality drastically. The resulting $\chi^2 = 1.47$ for 97 degrees of freedom, and for the column density we got $N_H = (1.01 \pm 0.19) \times 10^{20}\,\mathrm{cm}^{-2}$. The best fit black-body temperature $kT_{bb}^{\infty} = 43\,\mathrm{eV}$ appears to be the lowest value derived for any of the known XDINSs (see parameters in Table 1).

THE SYNCHROTRON EMISSION MODEL

The plasma emission model proposed in the present paper was recently applied to explain the X-ray spectra of RX J1856.5-3754 and RBS1774, revealing good fit quality in both cases [4, 5]. We performed fitting of the model spectrum Eq. (16) absorbed by cold interstellar matter with the EPIC-pn spectra of RX J0420. The best-fit results were $b = 1.27$ and $\epsilon_m = 0.1$keV, corresponding to $\chi^2 = 1.51$ for 96 degrees of freedom. The column density N_H, ϵ_m and b were treated as free parameters common to all three spectra. Only normalization was allowed to vary freely for different spectra independently, as was done in previous cases when the black-body model was applied. The fit results are listed in Table 1.

DISCUSSION

The spectral analysis of the pulse phase-averaged X-ray spectra of RX J0420 shows that the quality of the fits in the cases of both models (black-body and plasma emission models) is not very good. When looking at Fig. 1, one might consider the residuals around 0.3 keV as an absorption feature. This feature, described as a broad ($\sigma = 70\,\mathrm{eV}$) Gaussian absorption line, was noted and discussed by [9]. We added the absorption line at ~ 0.3 keV to both models considered in the present work and re-fit the data. The fit quality improved in both cases, provided an absorption edge model was used. The best-fitting energy of the edge is $E_{\mathrm{edge}} \approx 0.3$ keV, and the optical depth $\tau_{\mathrm{edge}} \approx 0.7$ (see Table 1). The resulting value of χ^2 reduces to 1.1 for both models.

The nature of the spectral features discovered in X-ray spectra of XDINSs is not fully clarified as of yet. According to the thermal emission scenarios, the most likely interpretation of the absorption lines is that they appear as a result of proton cyclotron resonance. The proton cyclotron absorption line at ~ 0.3 keV implies the magnetic field of $B_{\mathrm{cyc}} = 6.6 \times 10^{13}$ G, which differs from the value of the dipolar magnetic field inferred from the timing measurements $B_{\mathrm{dip}} = 1.0 \times 10^{13}$ G [10].

We suppose that existence of the absorption feature in X-ray spectra of RX J0420 might be caused by wave damping at photon energies ~ 0.3 keV, which takes place near the light cylinder. During the farther motion in the pulsar magnetosphere, the X-ray emission might come in the cyclotron damping range. If we assume that damping happens on the left slope of the distribution function of primary beam electrons (see Fig. 1 from [1]), the photon energy of damped waves will be $\epsilon_0 = (h/2\pi)2\omega_B/\gamma_b\psi^2 \simeq 0.3$ keV [4]. Taking into account the shape of the distribution function of beam electrons, we interpret the large residuals around ~ 0.3 keV as an absorption edge.

Despite the fact that fit quality considerably improves when including the absorption edge at 0.3 keV for both emission models, the physical interpretation of this feature is still uncertain. It might be caused by calibration uncertainties. A feature of possibly similar origin was detected in EPIC-pn spectra of the much brighter prototypical object RX J1856.4-3754 and classified as a remaining calibration problem by [10]. Thus, we agree that more data are necessary

to definitely prove or disprove the existence of this feature.

According to the fit results (see Table 1) the spectral analysis of the measured EPIC-pn X-ray spectra of RX J0420 does not seem to be enough to distinguish between the black-body and the plasma emission models. In contrast to the thermal radiation models, which appear to be somehow artificial, our scenario is based on a self-consistent theory. According to works [21] and [22] due to the cascade processes of a pair creation the pulsar's magnetosphere is filled with electron-positron plasma with the anisotropic one-dimensional distribution function. The beam particles undergo a drift perpendicular to the magnetic field due to the curvature of the field lines. Both of these factors (the one-dimensionality of the distribution function and the drift of particles) might cause the generation of eigen modes in the electron-positron plasma, if the condition of cyclotron resonance is fulfilled. The generated waves interact with the resonant electrons via the QLD, which leads to the diffusion of particles along and across the magnetic field lines, and inevitably causes creation of pitch angles by resonant particles. Therefore, the resonant electrons start to radiate in the synchrotron regime.

The estimations show that for the beam electrons with the average Lorentz-factor $\gamma_b \sim 10^7$, the synchrotron radiation comes in the same domain as the measured X-ray spectrum of RX J0420. Differently from the standard theory of the synchrotron emission [7], which only provides the power-law spectrum, our approach gives the possibility to obtain different spectral energy distributions. In the standard theory of the synchrotron emission, it is supposed that the observed radiation is collected from a large spacial region in various parts of which, the magnetic field is oriented randomly. Thus, it is supposed that along the line of sight of an observer the magnetic field directions are chaotic. In our case the emission comes from the region of the pulsar magnetosphere where the magnetic field lines are practically straight and parallel to one another. And in contrast to standard approach, we take into account the mechanism of creation of the pitch angles, which inevitably restricts their possible values.

ACKNOWLEDGEMENT

The authors are grateful to Prof. George Machabeli for valuable discussions. The HEASARC online data archive at NASA/GSFC has been used extensively in this research. This research was supported by the Shota Rustaveli National Science Foundation grant (12/31).

REFERENCES

[1] Arons J. 1981, ESA Special Publication, 161, 273
[2] Bekefi G. & Barrett A. H. 1977, *'Electromagnetic vibrations, waves and radiation'*, The MIT Press, Cambridge, Massachusetts and London, England
[3] Beskin V. S. 2010, *'MHD Flows in Compact Astrophysical Objects'*, Springer-Verlag, Berlin, Heidelberg
[4] Chkheidze N. 2011, A&A, 527, A2
[5] Chkheidze N. 2012, New Astronomy, 17, 227
[6] Dyks J. & Rudak B. 2000, A&A, 362, 1004
[7] Ginzburg V. L. 1981, *'Theoretical physics and astrophysics'*, Nauka, Moskva
[8] Goldreich P. & Julian W. H. 1969, ApJ, 157, 869
[9] Haberl F., Motch C., Zavlin V. E. et al. 2004, A&A, 424, 635
[10] Haberl F. 2007, Ap&SS, 308, 181
[11] Ho W. C. G., Kaplan D. L., Chang P., van Adelsberg M., Potekhin A. Y. 2007, MNRAS 375, 281
[12] Kazbegi A. Z., Machabeli G. Z. & Melikidze G. I. 1992, in *IAU Colloq. 128: Magnetospheric Structure and Emission Mechanics of Radio Pulsars*, eds.: Hankins T. H., Rankin J. M. & Gil J. A., Pedagogical Univ. Press, 232
[13] Kontorovich V. M. & Flanchik A. B. 2013, JETP, 116, 80
[14] Lominadze J. G., Machabeli G. Z. & Usov V. V. 1983, Ap&SS, 90, 19
[15] Machabeli G. Z. & Usov V. V. 1979, Soviet Astronomy Letters, 5, 238
[16] Malov I. F. & Machabeli G. Z. 2002, Astron. Rep., 46, 684
[17] Mignani R. P., Falomo R., Moretti A. et al. 2008, A&A, 488, 267
[18] Motch C., Zavlin V. E. & Haberl F. 2003, A&A, 408, 323
[19] Osmanov Z., Shapakidze D. & Machabeli G. 2009, A&A, 503, 19
[20] Pons J. A., Walter F. M., Lattimer J. M. et al. 2002, ApJ, 564, 981
[21] Sturrock P. A. 1971, ApJ, 164, 529
[22] Tademaru E. 1973, ApJ, 183, 625
[23] Van Kerkwijk M. H. & Kulkarni S. R. 2001, A&A, 378, 986
[24] Vedenov A. A., Velikhov E. P. & Sagdeev R. Z. 1961, Soviet Physics Uspekhi, 4, 332

Table 1: Model-Fit spectral parameters of RX J0420.0-5022 for combined fits to the EPIC-pn spectra obtained from individual observations in the energy interval $0.15 - 1.0$ keV.

Model	N_H (10^{20} cm^{-2})	ϵ_m (keV)	b	kT_{bb}^{∞} (eV)	$E_{\rm edge}$ (keV)	$\tau_{\rm edge}$	χ^2(d.o.f.)
`plasma`	$1.00^{+0.28}_{-0.28}$	0.10 ± 0.04	1.27 ± 0.31				1.51(96)
`plasma*edge`	$1.00^{+0.37}_{-0.37}$	0.10 ± 0.05	1.27 ± 0.42		$0.30^{+0.01}_{-0.01}$	$0.68^{+0.30}_{-0.30}$	1.10(94)
`bbody`	$1.01^{+0.19}_{-0.19}$			43.3 ± 1.2			1.47(97)
`bbody*edge`	$1.01^{+0.33}_{-0.33}$			46.3 ± 1.8	$0.31^{+0.02}_{-0.02}$	$0.69^{+0.21}_{-0.21}$	1.10(95)

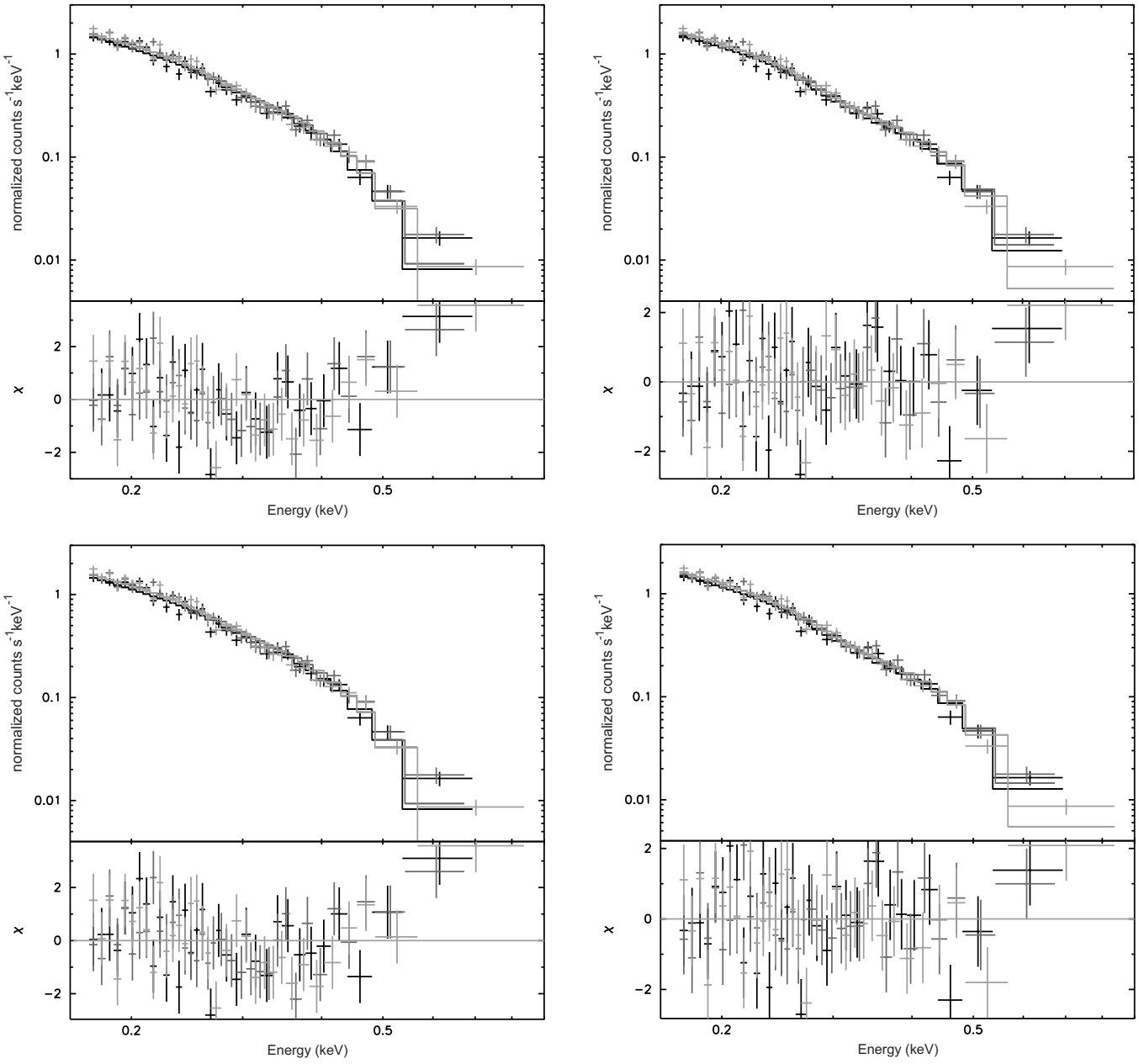

Fig. 1: Combined EPIC-pn spectra of RX J0420.0-5022. Top left: The absorbed black-body model fit. Top right: The black-body model fit including an absorption edge at ~ 0.3 keV. Bottom left: The synchrotron emission model fit absorbed by cold interstellar matter. Bottom right: Model fit including absorption edge at 0.3 keV.